GRATE Multi-Element Antenna for Accurate GNSS Measurements

J.A. Kegel[1,5], M.J. Arts[1,5], P. Benthem[1], M.J. Bentum[1,5], N. Bni Lam,[4], K. Blaauw[3], D. Boersma[1], A.J. Boonstra[1], A. Bos[2], P. Crosta[4], P. Donker[1], K. Drost[2], J.J.P. van Es[3], G. Fois[2], O. de Haas[2], J.E. Hargreaves[1], J. Herrewijnen[1], L. Hiemstra[1], P. Kruger[1], S. Kuindersma[1], A. Kuijt[2], S.P. van der Linden[2], H. van der Marel[1], M. Mevius[1], E. Meyer[5], J. Parro[4], J. Rijnsdorp[2], S. Yatawatta[1], A. Young[2]
[1]*Netherlands Institute for Radio Astronomy (ASTRON),* [2]*Science and Technology (S&T),*
[3]*Royal Netherlands Aerospace Centre (NLR),* [4]*European Space Agency (ESA ESTEC),* [5]*Eindhoven University of Technology*
[1]Dwingeloo, [2]Delft. [3]Marknesse, [4]Noordwijk, [5]Eindhoven, The Netherlands
j.a.kegel@tue.nl, ORCID 0009-0009-8125-5833

***Abstract*—The GRATE multi-element compact L-band antenna array and receiver is a system aimed at optimizing GNSS received signal quality by minimizing radio frequency interference and multipath. This system overview includes objectives, antenna and digital receiver architectures, and processing approaches for creating both fixed, and adaptive antenna beamshapes. System capabilities are demonstrated via simulation and initial field tests.**

***Index Terms*—GNSS, antenna array, beam-forming**

I. Introduction

The GRATE (GRound-station Array TEchnologies) prototype system is a multi-element antenna Global Navigation Satellite System (GNSS) receiver. The GRATE system is meant to be used for GNSS reference stations and for augmentation systems such as Wide Area Augmentation System (WAAS) and European Geostationary Navigation Overlay Service (EGNOS). It is aimed to provide resilient GNSS signal reception. It is specifically designed to handle adverse radio frequency environmental conditions such as Radio Frequency Interference (RFI) and multi-path. GRATE is a *smart* phased-array antenna in the sense it can adjust its properties according to changes in the radio frequency environment.

GRATE implements adaptive interference detection and mitigation/cancellation techniques, based on space-time and polarisation diversity, which identify and suppress pulsed and continuous interference. GRATE is specifically developed as Engineering Model at Technical Readiness Level (TRL) 5, and includes the full receiver chain. It is able to maximize code and carrier phase tracking performance while optimising received signal-to-noise-and-interference ratio according to the actual RF environment scenario (thermal noise, multipath and interference).

The GRATE antenna will be used for reception of the Right Hand Circular Polarized (RHCP) open signals of both the Galileo and GPS systems. The GNSS signals considered are E5/L5 and E1/L1 centered respectively at 1176.45 and 1575.42 MHz. The signals of the individual satellites are identified using a Pseudo Random Number (PRN) that is modulated on the satellites signal. Figure 1 shows the GRATE prototype system during anechoic room tests.

979-8-3503-5685-4/24/$31.00©2024 European Union

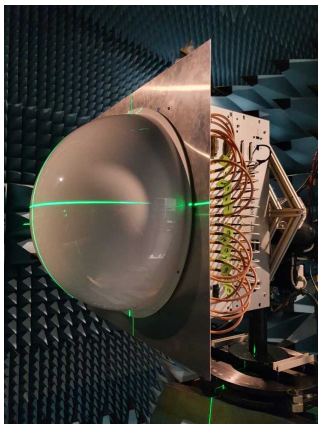

Fig. 1. GRATE phased-array antenna with radome, the antenna front-end unit, and the antenna processor in the ASTRON anechoic room during laser assisted alignment.

Descriptions of antennas with similar capabilities also intended for reference station applications can be found in, *e.g.*, [8] and [9].

This paper is organized as follows. The first section describes the antenna system architecture composed of the antenna elements, the antenna front-end electronics, the antenna processing and the GNSS receiver. Next, the simulation is described related to the antenna as well as the antenna processing. Then initial measurement results are briefly given and the conclusions and future work is presented. Finally we acknowledge the funding organisation.

II. Architecture

A main aspect in obtaining resilience is optimal design ensuring the system remains linear in both the analogue and digital domains for the expected RF environment, especially strong signal interference conditions, and for reasonable cost. A second important element in achieving resilience is utilizing spatial beam-forming using seven dual-polarization antenna

elements. The beam-former optimizes beam-shapes for GNSS satellite signal reception using the so-called Fixed Reception Pattern Array (FRPA) mode. The system is also able to place spatial nulls in directions of interfering signals. This mode is called the Controlled Reception Pattern Array (CRPA) signal reception mode. Finally, the GNSS receiver implements several beam-formed time-series interference mitigation approaches, such as adaptive notch filtering (ANF).

The GRATE architecture supporting the functionality mentioned above is shown in Figure 2 with the seven dual-polarization antennas (top) and the top-level structure of GRATE (bottom) consisting of four functional blocks that are detailed in the following subsections.

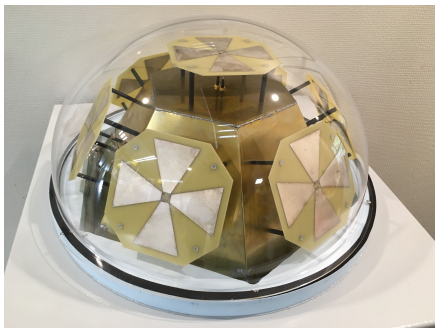

(a) GRATE seven dual-polarization antennas

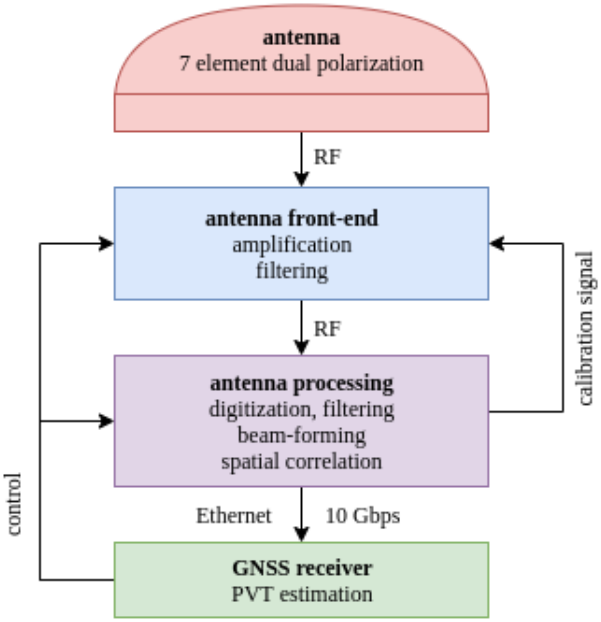

(b) GRATE top-level system architecture

Fig. 2. GRATE antenna element configuration GRATE top-level architecture, with antenna array signals conditioned in the antenna front-end, followed by a beam-forming stage, and PVT estimation in the GNSS receiver. Indicated also are the control lines and the calibration signal paths.

A. Antenna

The GRATE antenna consists of a seven element L-band dual polarization bow-tie phased-array antenna, with six antennas uniformly distributed on a 44.6 cm diameter hemisphere with a central antenna located on top. The six tilted antenna elements improve signal quality for low elevation signals. This optimizes interference mitigation by spatial filtering close to the horizon. Each element is capable of simultaneously receiving L1/E1 and the L5/E5a frequencies within the 1100-1600 MHz RF input frequency band.

Pair-wise combining concentric antenna elements into RHCP and LHCP signals is realised in the digital domain in the antenna processing unit. The reason is that digital signal processing of fourteen element signals provides more degrees of freedom for beam-shape tuning than seven antenna signals would provide, as shown by [2]. These additional degrees of freedom can be used to form deeper nulls (increasing the interference subspace to be suppressed), or to increase the number of nulling directions. Having both orthogonal polarised signals available for further digital signal processing allows examining the electromagnetic polarisation properties from the interfering signal.

B. Antenna front-end

The aim of the analog front-end is to condition the input signals in order to comply with the Analogue-to-Digital Converter (ADC) dynamic range requirements while optimizing the system noise performance for the required GNSS frequency bands. This includes low-loss GNSS passband filters, a low noise (NF $\leq$ 1 dB) with high dynamic range ($OP_{-1dB} \geq 20$ dBm) first signal gain stage, a GNSS frequency band selection stage, buffer amplifiers with two-bit controlled discrete step attenuators to provide Automatic Gain Control (AGC), and finally the anti-aliasing filters. It also includes a calibration (equalizer) input signal coupler. Internally, the ADC provides a fast response input attenuator to prevent damage due to possible excessive signal power levels. Given the analogue front-end gain, activation of this attenuator affects the system noise figure by 0.7 dB. All signal interfaces are designed for 50 Ω.

C. Antenna processing

The antenna processing unit is based on a Xilinx System on Chip system[1] that includes a Field Programmable Gate Array (FPGA). This SoC conveniently includes sixteen 14-bit Analogue to Digital Converters (ADCs), with a switchable input attenuator. The sampling frequency is 2 G samples per second (Gsps), allowing capturing the GNSS bands in the second Nyquist zone. After down-conversion in the RF SoC, the signals are further processed in the FPGA.

The system processes two GNSS bands simultaneously, and combines all fourteen antenna element signals in a beam-former stage, capable of generating RHCP and LHCP output signals. Care is taken to ensure the phase information between the input bands is maintained. The beam-formed signals are re-quantized to eight bits and sent to the GNSS receiver stage via a 10 Gbps Ethernet stream.

[1]Xilinx Zynq UltraScale+ RFSoC ZCU216 System-on-Chip (SoC) evaluation board

In addition to beam-formers, the FPGA also accommodates a signal equalization (calibration) stage. The equalisation training sequence is designed for minimal interference to the wanted GNSS signals. This spread-spectrum signal covers the full pass-band and is synchronous between the two sampled GNSS frequency bands. This calibration signal is generated using the on-chip Digital to Analogue Converters (DACs), and fed to the antenna front-end.

The FPGA antenna spatial 14×14 signal correlator is implemented to estimate the correlation matrix subspace structure as input to the CRPA beam-former mode. The nulling filters and DoA estimates are derived from these correlation matrices. The FPGA utilisation is about 90%, with the equalizer being the biggest component. Adding more bands would require adding SoCs.

D. GNSS receiver

The GNSS receiver and control unit receives the beam-formed (10 GBit ethernet) data stream to compute the relevant GNSS observables, to check the input signals, and to control the antenna. The main components of the GNSS receiver and control unit are:

- the GNSS receiver (Rx) to acquire and track the satellite signals, and to compute the relevant Rx-observables (including, code phase, carrier phase, C/N0 and Doppler shift) and the resulting PVT values,
- interference detection on the beam-formed signal and generating an alarm if such an event is found, and
- computing the antenna beam-former weight coeffcients based on the spatial correlator output.

The GNSS receiver used is based on an open source GNSS-SDR receiver [3]. It is able to acquire, track and decode most (public) GNSS signals, including Galileo E1, E5A, GPS L1, L5, GLONASS and BeiDou. Derived pseudo ranges from the different signals are combined in a uniform Position, Velocity, and Time (PVT) determination block. Much of the data resulting from the processing chain, such as carrier-to-noise ratios and GNSS observables (pseudo range, carrier phase) can be retrieved in real-time from the application via a serialised connection, or dumped to files in standardised formats such as MATLAB, RINEX 2/3 and NMEA. Configuration of the software is done through text-based configuration files.

III. Simulation

GRATE system simulations include antenna element RF simulations using ANSYS HFSS, and system response simulations using Python, based on simulated or measured element responses.

A. FRPA beam mode

The fourteen HFSS simulated antenna element responses are obtained with an azimuth step size of 5°, an elevation step size of 2°, and for six frequencies uniformly spaced in the range 1.1 to 1.6 GHz. The HFSS simulations do take cross-talk (mutual coupling) into account. The FRPA array responses are simulated using Python, and use the HFSS element response data sets as input. Figure 3(a) shows the FRPA beam response for E5/L5 for RHCP GNSS signals. This FRPA beam-former coefficients were estimated using a strong source at zenith. Zenith is at the centre, the horizon is indicated by the white circle, with nadir at the outer rim. The spatial sidelobes between the horizon and nadir are roughly at the -20 dB level.

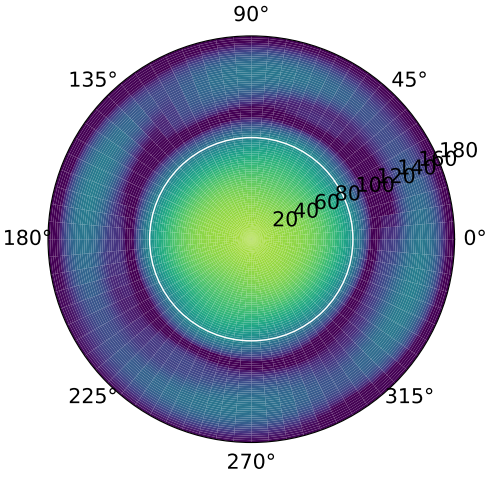

(a) E5/L5 FRPA beam

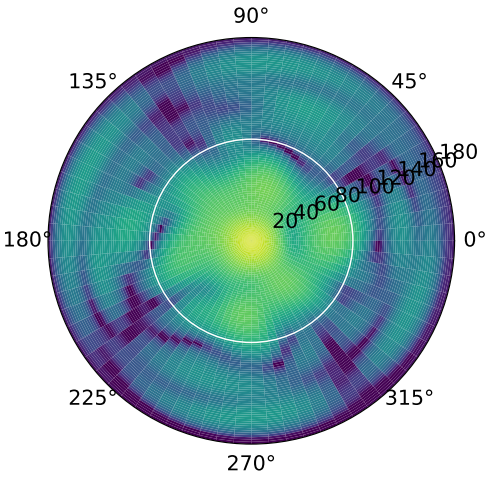

(b) E1/L1 CRPA anti interference beam

Fig. 3. FRPA MVDR E5/L5 Nominal Beam response to RHCP signals with zenith at the centre (with 11.5 dBi gain), the horizon indicated by the white circle, and nadir at the outer rim. E1/L1 CRPA beam with two nulls near the horizon at 65° and 170°.

B. Beam-forming and interference suppression

Figure 3(b) shows interference nulling capability for E1/L1. Given the Direction of Arrival (DoA) of the interfering signals, a projection filter matrix $\mathbf{P}$ was crated and applied to the beam-former and to the simulated correlation matrix. The projection matrix $\mathbf{P}$ is applied to an FRPA beam-former weight vector

$\mathbf{w}_{frpa}$ thus forming a modified filtered CRPA weight vector $\mathbf{w}_{crpa}$ with $\mathbf{w}_{crpa} = \mathbf{P}\mathbf{w}_{frpa}$. The correlation matrix is created using 500000 time samples from GNSS data files, and using receiver Gaussian channel noise $T_{sys} = 550K$. As the correlation matrix and beam-former are based on 14 single antenna elements rather than 7 dual polarisation antennas there are enough degrees of freedom to suppress multiple interfering sources with the figure showing two nulls.

For FRPA and CRPA beam-forming, DoA estimation, and spatial filtering, multiple approaches have been assessed. Simulated beam-formers include Bartlett, MVDR, MUSIC, and nonlinear Least Squares in which beam-forming weights are found for a predefined set of desired beam responses. MVDR turned out to be very stable (satisfying beamformer weights were produced under a wide variety of conditions), MUSIC appeared not very stable, and as expected Bartlett beam-forming yields very wide beams not suitable for DoA estimation. Nonlinear Least Squares estimation was effective and stable as well, but for FRPA beam-forming it did not outperform MVDR. Nulling was implemented via a spatial correlation matrix subspace analysis or using DoA estimates, and projection filtering.

IV. Initial measurements

Initial measurements of the GRATE system were done in an anechoic room shown in figure1. With the antenna size and bandwidths used, the RF source in the room can be considered to be located in the far field (for most of the tests). The measured element responses (not shown here) appeared to be very similar to the simulated ones.

Figure 4 shows the Minimum Variance Distortionless Response (MVDR) response to an RF source in the anechoic room. The figure was constructed by measuring the 14×14 correlation matrix $\mathbf{R}$ for a fixed antenna orientation, and by subsequently

computing the beam-formed power $\mathbf{w}'(\theta,\phi)^H \mathbf{R}\mathbf{w}'(\theta,\phi)$ for the different (θ,ϕ) values for the weight vector $\mathbf{w}'$. The source can be seen in direction $(\theta,\phi) = (45°, 30°)$.

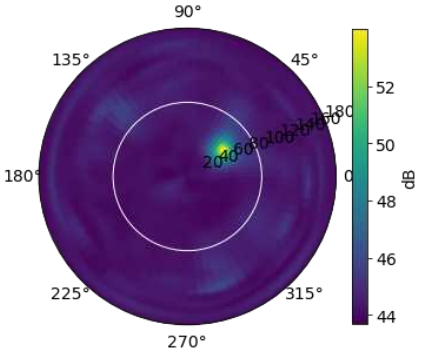

Fig. 4. MVDR response to a RF source in the anechoic chamber at (θ,ϕ) = (45°,30°), based on recorded output data from the (spatial) interference correlator.

V. Conclusions and future work

The aimed Technical Readiness Level for the GRATE system under development is five. The system is housed in an outdoor cabinet, and weeks of outdoor monitoring at ASTRON showed a stable GNSS signal reception capability under varying environmental conditions. Simulations indicate that the system in principle should be capable to simultaneously detect and suppress multiple interfering sources. Direction of Arrival estimation of coherent Radio Frequency Interfering sources tends to be more difficult than for non-coherent sources, but as the spatial nulling filters are based on a subspace analysis, coherent radio frequency interference can be nulled as well. Initial measurements at ASTRON have shown that the measurements are very similar to the simulations.

Antenna element tests, beam-former tests, and phase centre measurements are currently being conducted at the Royal Netherlands Aerospace Centre using a shielded anechoic room. These tests include measuring phase centre behaviour as a function of frequency and Direction of Arrival. Field tests at the outdoor Antenna Test Range (ATR) are scheduled as well, and are aimed at demonstrating nominal operation under different interference scenarios. Subsystem environmental test (thermal) have been conducted at ASTRON.

Future work will investigate how the creation of nulls in the antenna pattern will affect the delay characteristics of the front-end, and thus the carrier phase, as function of elevation and azimuth.

Furthermore, it would include boosting the Technical Readiness Level. The GRATE antenna forms an excellent reference point on which further developments can be based.

Acknowledgment

This activity is funded by the EU. ESA has received funds in its quality as funding body under the European Union's Horizon 2020 research and innovation programme.

The work presented in this document was conducted under ESA contract with reference AO/2-1689/18/NL/AS - H2020-ESA-015 WO1 GNSS Reference Station Receiver Technologies.

Disclaimer

The view expressed herein can in no way be taken to reflect the official opinion of the European Union and/or the European Space Agency. Neither the European Union nor the European Space Agency shall be responsible for any use that may be made of the information it contains.

References

[1] Shahrzad Afroozeh et al., *Antiference: New Concept for Evolutive Mitigation of RFI to GNSS* in Proceedings of the European Navigation Conference 2023, Noordwijk, Zuid-Holland, 31 May–2 June 2023, MDPI: Basel, Switzerland, doi:10.3390/ENC2023-15451

[2] Kwansik Park, Dongkook Lee, and Jiwon Seo, "Dual-polarized GPS antenna array algorithm to adaptively mitigate a large number of interference signals," *Aerospace Science and Technology*, vol. 78, pp. 387–396, 2018.

[3] C. Fernańdez-Prades et al., "An open source Galileo E1 software receiver," 2012 6th ESA Workshop on Satellite Navigation Technologies (Navitec 2012) & European Workshop on GNSS Signals and Signal Processing, Noordwijk, Netherlands, 2012, pp. 1-8, doi: 10.1109/NAVITEC.2012.6423057.

[4] A.J. Jahromi et al., "Galileo signal authenticity verification using signal quality monitoring methods," in 2016 International Conference on Localization and GNSS (ICL-GNSS), 2016, pp. 1–8.

[5] A.J. Jahromi, "GNSS Signal Authenticity Verification in the Presence of Structural Interference (Unpublished doctoral thesis), University of Calgary, Calgary, AB., 2013, http://hdl.handle.net/11023/927, doi:10.11575/PRISM/26310

[6] A. Broumandan, R. Siddakatte and G. Lachapelle, "An approach to detect GNSS spoofing," in *IEEE Aerospace and Electronic Systems Magazine*, vol. 32, no. 8, pp. 64-75, Aug. 2017, doi: 10.1109/MAES.2017.160190.

[7] D. Akos et al., *GNSS software defined radio: History, current developments, and standardization efforts*, Proceedings of the 35th International Technical Meeting of the Satellite Division of The Institute of Navigation (ION GNSS+ 2022), Denver, Colorado, Sep. 2022, pp. 3180–3209.

[8] Konovaltsev, Andriy, et al., *Development of Array Receivers with Anti-Jamming and Anti-Spoofing Capabilities with Help of Multi-Antenna GNSS Signal Simulators*, Proceedings of the 32nd International Technical Meeting of the Satellite Division of The Institute of Navigation (ION GNSS+ 2019), Miami, Florida, September 2019, pp. 953-966. https://doi.org/10.33012/2019.16988.

[9] N. Pastori et al., *Multi Element Antenna Technology for Robust GNSS Reference Stations*, NAVITEC 2022, Noordwijk, Netherlands, 2022.